NATIONAL ADVISORY COMMITTEE FOR AERONAUTICS

TECHNICAL NOTE 2406

APPLICATION OF X-RAY ABSORPTION TO MEASUREMENT OF SMALL AIR-DENSITY GRADIENTS

By Ruth N. Weltmann, Steven Fairweather and Daryl Papke

Lewis Flight Propulsion Laboratory
Cleveland, Ohio

Washington
July 1951

NATIONAL ADVISORY COMMITTEE FOR AERONAUTICS

TECHNICAL NOTE 2406

APPLICATION OF X-RAY ABSORPTION TO MEASUREMENT OF SMALL AIR-DENSITY GRADIENTS

By Ruth N. Weltmann, Steven Fairweather and Daryl Papke

SUMMARY

An analysis of two X-ray absorption methods for determining small air-density gradients is presented. One method utilizes a Geiger-Mueller counter for detection and the other uses photographic film for detection. The methods are a refinement of a previous similar application. With the resulting sensitivity in density measurement, the first method was successfully applied to the evaluation of a 6-percent density gradient of a flat-plate boundary layer of about 0.024-inch thickness in a two-dimensional-flow channel.

In the other method, the divergence of the X-ray beam passing the absorber poses a problem. A solution to this problem is postulated. In addition, example calculations of the expected sensitivity in boundary-layer density measurements are given for X-ray parameters selected for optimum operation.

INTRODUCTION

The application of soft X-ray absorption as a technique for the determination of air densities has a potential advantage over the optical radiation methods, especially in determining air densities over a long path length, in that X-ray refraction errors are reduced by at least a factor of 10^3. In addition, all radiation methods have the advantage that no probes have to be inserted into the stream when evaluating density gradients in a wind tunnel. Radiation methods, however, can only be employed when two-dimensional flow can be presupposed. In references 1 and 2, the possibilities of the X-ray absorption method are recognized and are applied to the investigation of densities in wind tunnels (reference 1) and shock waves in supersonic flow (reference 2). All investigators using this method concluded that the full potential of the X-ray absorption method can only be realized if the probing X-ray beam can be made substantially smaller

than that used in references 1 and 2 by providing an X-ray source of higher intensity and an X-ray detector of higher sensitivity.

A study of two different X-ray detecting methods was made at the NACA Lewis laboratory and the results and the conclusions obtained are presented herein. The sensitivity of the air-density measurement can be increased fourfold, even though the probing X-ray beam would be decreased in size by a factor of 30 with reference to the instrument previously described (references 1 and 2) by employing Geiger-Mueller counters instead of an ionization chamber to provide a detector with increased sensitivity and by utilizing a tungsten-target X-ray tube instead of one with a chromium target to increase the X-ray intensity. With a resulting sensitivity in air density of ±1.5 percent at atmospheric pressure and a probe width of 0.002 inch, this method can be applied to density determinations in a boundary layer of an airfoil. The density gradient at one station in the boundary layer of a flat plate at subsonic flow of Mach number of 0.55 was experimentally determined by X-ray absorption measurements and compared with a calculated laminar boundary layer to indicate the feasibility of the X-ray-absorption method for such studies.

Employing photographic film as an X-ray detector permits the analysis of a complete boundary-layer station from a single exposure without loss in sensitivity in air-density measurement. This usage eliminates the machining of accurate and movable parts, which are required in the point-by-point method. In the case of X-ray detection by photographic film, each individual ray acts as a probing element. The resolution of the measurement, however, is determined by the geometry of the setup and by the size of the densitometer pickup used to measure the film densities.

The X-ray beam exhibits a conical geometry; this divergence of the beam should pose no problem when employing Geiger-Mueller counters with an X-ray beam receiving slit of 0.002 inch width or a scanning X-ray beam with photographic film as the detector. For the single-exposure photographic method, however, the measured X-ray intensity must be corrected for the divergence of the X-ray beam. Suggestions for applying such corrections are presented.

Operating characteristics required when using X-ray equipment with Geiger-Mueller counters and photographic film for air-density measurements in a boundary layer of an airfoil at given flow conditions are calculated.

THEORY AND DESCRIPTION OF METHOD

The intensity I of an X-ray beam remaining after absorption is given by Lambert's law

$$\frac{I}{I_0} = e^{-B\rho L} \tag{1}$$

where

I_0 initial X-ray intensity

B total mass absorption coefficient

ρ density of gas

L path length through absorbing gas

(For convenience, all symbols are defined in appendix A.) This law presupposes that the initial X-ray beam is directly incident on the absorbing medium and that the source consists of parallel rays. If, however, the initial X-ray source is a point source and a distance d away from the detector, equation (1) becomes

$$\frac{I}{I_0} = \frac{CA}{4\pi d^2} e^{-B\rho L} \tag{2}$$

where the constant C is a function of the absorption that the initial X-ray beam experiences before entering and after leaving the absorber and A is the cross-sectional area of the X-ray beam at the distance d, as shown in figure 1.

The sensitivity in air density is calculated from equation (2) as

$$\frac{d\rho}{\rho} = -\frac{dI}{IBL\rho} \tag{3}$$

and the minimum detectable density change can be expressed as

$$\Delta\rho = \frac{\log_e\left(1 - \frac{\Delta I}{I}\right)}{BL} \tag{4}$$

which converts to equation (3) for

$$\left|\frac{\Delta I}{I}\right| \ll 1$$

In this equation, $\Delta I/I$ represents the accuracy in intensity measurement.

From equation (2), it is seen that the number of quanta entering the detecting device depends not only on the density of the absorber but also on the length of the absorbing path, the geometrical arrangement of the equipment, the cross-sectional area of the X-ray probing beam, the initial X-ray intensity, and the mass absorption coefficient. A study of these variables shows that:

1. The absorber length is invariant in any given problem.

2. The geometrical arrangement of the equipment should be such that the loss in X-ray intensity between the X-ray source and the absorber is a minimum. In the case where the mechanical geometry requires that the X-ray tube be mounted a given distance from the section containing the absorbing medium, this distance is kept as small as feasible and the loss in intensity due to absorption is minimized by passing the X-ray beam through an evacuated tube. Especially thin windows are employed at the entrance and exit sides of the absorber section for least intensity losses. In special cases, demountable X-ray tubes may be employed to altogether eliminate window material.

3. The cross-sectional area of the probing X-ray beam is chosen to be a minimum for highest resolution but sufficient in size to give the intensity required by the detector for desired accuracy.

4. A high initial X-ray intensity is desired to obtain a maximum X-ray flux for high detecting sensitivity and short time measurements. The initial X-ray intensity increases directly with the atomic number of the target material and the applied current and is a function of the applied voltage, as shown in figure 2. The tungsten-target X-ray tube, because of its higher atomic number, generates higher intensities than the iron-target tube. The intensity values in figure 2 were measured through the beryllium window of the X-ray tubes and at a fixed distance; hence the values are not absolute but rather are representative of relative intensities. The maximum value of the intensity is limited by the target material available in commercial X-ray tubes, by the current limitations set by the X-ray equipment, and by the maximum voltage that can be applied without loss in the desired sensitivity in the air-density measurement, as will be explained later.

5. The mass absorption coefficient is selected to permit sufficient flux to reach the detector so as to approach the desired sensitivity in air-density measurement. The total mass absorption coefficient for monochromatic X-rays, in this case for the effective wavelengths of the generated continuous spectra, equals

$$B = \frac{KZ^4}{V^3} + S \approx \frac{C'}{V^3} \qquad (5)$$

where S is a term due to scattering, which can be neglected because it never exceeds 0.1 percent for the soft X-rays employed in measuring air-density gradients and Z is the atomic number of the absorber, which is air in this study. Thus equation (5) indicates that the mass absorption coefficient is inversely proportional to the third power of the voltage, where the voltage is inversely proportional to the effective wavelength of the applied X-rays. After the proportionality constant C' was experimentally obtained from two determinations of the mass absorption coefficient at 3.2 and 4.0 kilovolts, approximate mass absorption coefficients were calculated for several voltages and are plotted in figure 3.

For high sensitivity in air-density measurements, according to equation (3), a high mass absorption coefficient is desired and can be achieved by employing low voltages. A high intensity is also required to give sufficient counting accuracy and can be obtained by applying high voltages. The voltage is therefore adjusted to give sufficient X-ray intensity and a mass absorption coefficient for highest sensitivity in air-density measurement.

SENSITIVITY OF DENSITY DETERMINATION

Because the sensitivity of the density measurements is of prime importance for the evaluation of density gradients, its limitation is analyzed for the two selected X-ray intensity detecting methods of employing the G-M (Geiger-Mueller) counter and, subsequently, the photographic film as receiving element.

Geiger-Mueller Counter as Detector

Counter resolving time. - For measuring the air densities by means of X-ray absorption, G-M counters were used with a scaling circuit, which allows simple handling and produces stable operating conditions. Not only are G-M counters more sensitive than ionization chambers, but also their sensitivity does not change with a variation in wavelength. Each quantum, independent of the X-ray energy, entering the counter produces a pulse that after suitable amplification will trigger the scaling circuit. If, however, the quanta are following each other at shorter intervals than the resolving time τ of the counter permits, a counting error equal to $R_m\tau$, where R_m is the measured counting rate, is introduced. The true counting rate n can be obtained as follows:

$$n = \frac{R_m}{1-R_m\tau} \tag{6}$$

The counter resolving time varies for each counter, but was experimentally found to be 5.7×10^{-6} minutes on the average. This counter resolving time introduces an error of about 0.6 percent for a counting rate of 1000 counts per minute and is less for lower counting rates.

Counting sensitivity. - The X-ray quanta entering the G-M counter are randomly distributed. The counting of such randomly distributed pulses introduces an error due to the law of statistics. This relative probable error $\Delta N/N$ is given as:

$$\frac{\Delta N}{N} = \pm \frac{0.67\sqrt{N+N_B}}{N-N_B} \tag{7}$$

where N is the total number of counts and N_B is the number of background counts, which are always present. The number of counts due to the quanta emanating from the X-ray source is $N - N_B$, where N_B can be neglected when $N \gg N_B$. This condition exists for a short-duration high-intensity count, such as is desirable for measurements of dynamic wind-tunnel conditions. The background count N_B for a counting period of 1 minute was found to be about 40 to 50. For a duration of measurement of 1, 2, and 3 minutes and a counting rate of 500 counts per minute, the relative probable error according to equation (7) is ±3.5 percent, ±2.5 percent, and ±2.0 percent. Hence, 500 counts per minute seem a required minimum intensity to give sufficient counting accuracy over short enough measuring periods.

Experimental method and results. - The accuracy in counting and the sensitivity in air-density measurement were experimentally investigated. A Machlett X-ray tube, Type A-2 Diffraction Tube, with a tungsten target and two separate 0.5-millimeter-thick beryllium windows was employed. The absorbing medium, air, was contained in a test section of 4-inch path length with a cellophane window (0.001 in. thick) on each side. The X-ray beam passed through the first cellophane window, the absorbing air, and the second cellophane window to the measuring G-M counter. The air density in the test section was changed by evacuation with the aid of a vacuum pump. The measured X-ray intensity varied over a ratio of 1 to 3 for about one-half atmosphere change in density for an applied X-ray tube voltage of 3.2 kilovolts and a resulting mass absorption coefficient of 90 square feet per pound. In order to eliminate the errors in the X-ray-intensity measurements resulting from fluctuations in the X-ray emission, a reference count with a second G-M counter attached directly to one window of

the X-ray tube was obtained. The ratio of the measuring and reference counts N/N_R is proportional to the intensity ratio in equations (1) and (2). The probable relative error of the ratio N/N_R is composed of the errors of both counts and can be expressed as

$$\frac{\Delta(N/N_R)}{N/N_R} = \pm\sqrt{\left(\frac{\Delta N}{N}\right)^2 + \left(\frac{\Delta N_R}{N_R}\right)^2} \tag{8}$$

The experimental counting accuracies of three reference ratios each obtained from ten measurements with the calculated values for the same number of counts are compared in the following table:

Experimental (averaged from 10 points)					Calculated (from equations (7) and (8))		
N_B	N_R	N	$\frac{N}{N_R}$	$\frac{\Delta(N/N_R)}{N/N_R}$	$\frac{\Delta N_R}{N_R}$	$\frac{\Delta N}{N}$	$\frac{\Delta(N/N_R)}{N/N_R}$
40	3,530	1,850	0.525	±2.02	±1.15	±1.61	±1.98
120	13,450	7,090	.525	±1.52	± .58	± .82	±1.03
200	19,600	10,260	.524	±1.54	± .54	± .69	± .87

From the preceding table, it seems that a counting accuracy of ±1.5 percent is about the best obtainable with the commercially available components. This accuracy is more than sufficient for the intended wind-tunnel applications.

With the described test setup and a counting accuracy of about ±2.0 percent, a sensitivity in air-density measurement of better than ±1.0 percent is obtained at atmospheric pressure (equation (3)). This sensitivity seemed suitable for application of the method to the density measurements of a boundary layer. Such an application will be described later in this report.

Photographic Film as Detector

Theory of film detector. - The characteristic curve of a photographic material, emulsion density as a function of the logarithmic exposure, is a straight line over a considerable portion. The equation of this line can be expressed as

$$D = \gamma\left(\log\frac{I}{A} + \log t - \log i\right) \tag{9}$$

where

D film density

γ slope of line

I intensity impinging on film, in this case X-ray intensity

t exposure time

i inertia of photographing material, constant of emulsion for fixed developing procedure

Substituting equation (2) in equation (9) gives

$$\left.\begin{aligned} D &= -0.434\ \gamma BL\rho + K' \\ \text{and} \\ \rho &= -\frac{D}{0.434\ \gamma BL} + K'' \end{aligned}\right\} \qquad (10)$$

where

$$K' = \gamma\left(\log \frac{I_0 C}{d^2} + \log t - \log i\right)$$

and

$$K'' = \frac{K'}{0.434\ \gamma BL}$$

Both K' and K'' are constant for a given experimental arrangement and exposure time. From equation (10), the sensitivity in air-density measurement is

$$\frac{d\rho}{\rho} = -\frac{dD}{0.434\ \gamma BL\rho} \qquad (11)$$

and a minimum detectable change in air density can be expressed as

$$\Delta\rho = \frac{\Delta D}{0.434\ \gamma BL} \qquad (12)$$

where ΔD represents the accuracy in emulsion-density measurement. Equations (11) and (12) are very similar to equations (3) and (4), only

the accuracy in counting intensity is substituted by the accuracy in the film-density measurement for any constant γ of the photographic material.

Experimental method and results. - In figure 4 is shown the characteristic curve of Kodak film Spectrum Analysis No. 1 for 4.0-kilovolt X-rays using Kodak Developer D-19 and a developing time of 5 minutes. Other photographic materials and developing procedures were investigated but were found less satisfactory. Figure 5 illustrates the experimental arrangement. The X-ray beam from the tungsten-target Machlett Type A-2 Diffraction tube passes through the 5.1-inch-long test section, through one 0.001-inch-thick cellophane window, and impinges on the photographic film. In order to obtain the characteristic curve in figure 4, the energy (IXt) incident on the photographic film was changed by varying the exposure time t while the X-ray intensity I remained constant. The emulsion densities within the straight portion of the characteristic curve range from 0.7 to 2.3. The slope of this line is $\gamma = 1.66$. For each given set of X-ray intensities determined by the parameters of the experiment and the measuring conditions, the exposure time is so selected as to keep the resulting emulsion densities within the range of the straight portion of the characteristic curve.

The setup in figure 5 was used to check equation (10) experimentally. The test section was evacuated to different air densities. A constant intensity X-ray beam of 4.0 kilovolts and 17.5 milliamperes was passed through the test section at each of the known air densities and the film was exposed for a predetermined time. The film densities were measured on a photographic analyzer with a pickup 0.063 inch in diameter. Three sets of measurements were made and are plotted in figure 6. The exposure time for each set of data was so adjusted as to keep the emulsion densities within the range of the straight portion of the characteristic curve. In order to normalize the three sets of data, equation (10) was changed to

$$\rho_m - \rho = \frac{(D-D_m)}{0.434\ \gamma BL} \tag{13}$$

where ρ_m was arbitrarily chosen to be the maximum density measured for each set of data and D_m is the emulsion density for the air density ρ_m. The dashed line in figure 6 is calculated from equation (13) for an experimental value of B of 46.6 square feet per pound and L of 0.425 foot. Figure 7 shows the photographic exposures corresponding to the experimental points of run 2 in figure 6.

In order to calculate the sensitivity of the air-density measurement, it is necessary to know the accuracy in the emulsion-density measurement. For this purpose a number of measurements were made at constant air densities, at fixed X-ray conditions and identical exposure times (about 45 sec). Three sets of data obtained at three air densities are shown in figure 8. The emulsion densities plotted on the graph were measured on the densitometer. The probable error in D was found to be ±0.006 and to be independent of the emulsion-density value. The probable error in emulsion density D was measured to be ±0.005 by a microphotometer with a slit pickup of 0.0004-inch width, which indicates approximately the same accuracy. The smaller size pickup of the microphotometer makes this instrument better suited to measurements of density gradients over the extremely short distances encountered in boundary layers and also where high resolution in density gradient is required. A probable error in D of ±0.006 results in a sensitivity in air-density measurement of ±0.6 percent at atmospheric density (equation (11)), which corresponds to a minimum detectable difference in air density of about 4×10^{-4} pound per cubic foot.

With the resulting sensitivity in air-density measurement of ±0.6 percent, the photographic method seems applicable to density determinations in a boundary layer. This arrangement has the advantage that a complete boundary-layer station is obtained from a single exposure, which eliminates the movable parts required for scanning in the previous method.

APPLICATION TO WIND TUNNEL BY USING GEIGER-MUELLER COUNTERS AS DETECTORS

Photographs of the tunnel, X-ray equipment, and detectors are shown in figure 9. Figure 10 is a cross-sectional drawing of the tunnel. A G-M counter directly connected to one window of a Machlett tungsten-target X-ray tube, Type A-2 Diffraction, measures the reference counts. The X-ray beam from the second window is passed through an evacuated chamber, a cellophane window, the tunnel section of 4-inch path length, and a second cellophane window to the measuring G-M counter. A receiving slit 0.002 inch in width and 0.25 inch in length is attached to the front of the detecting G-M counter in such a way that it, together with the G-M counter, can be rotated to be alined parallel to the airfoil. Because of the extremely small size of the receiving slit, it must be perfectly alined with regard to the model and the air stream. The airfoil is a flat plate 1 foot in length mounted on a micrometer arrangement that moves it back and forth in relation to the 0.002-inch probing X-ray beam. The X-ray probing beam is stationary

and traces the boundary layer at a position about $7\frac{3}{8}$ inches back from the leading edge of the plate. The tunnel had its maximum operational flow at a Mach number of 0.55 and was operated at near atmospheric density. An applied X-ray voltage of 3.2 kilovolts was chosen.

The calibration curve is given in figure 11. When modified from equation (2) for the reference method, the equation of this curve becomes

$$\frac{N}{N_R} = ke^{-B\rho L} \tag{14}$$

where k combines those intensity and absorption factors for both counts, which remain constant during each measurement. The calibration curve is obtained by evacuating the tunnel to various densities, which are determined from pressure-probe manometer readings recorded simultaneously with the counting-rate-ratio measurements. Once this curve is established for a given X-ray setup, it is necessary only to locate one point for each X-ray run because only k changes, which results in merely a parallel shift of the calibration line. The point establishing the parallel shift is best obtained from a counting-rate ratio corresponding to the free-stream density ρ_0, which is determined from pressure-probe measurements.

In order to compensate for the interference of the X-ray beam with the presence of the airfoil, X-ray-intensity curves were taken for each run without air flowing through the tunnel. In these compensating curves, the X-ray intensity is measured as a function of the distance of the plate surface from the X-ray beam. In a properly alined instrument, the intensity is unaffected when the plate surface is 0.001 inch and more removed from the slit. The experimental points in figure 12 are calculated from X-ray intensities that are corrected from compensating curves measured immediately prior to or after each tunnel run.

The plotted points in figure 12 are obtained from X-ray-absorption data, whereas the solid line is calculated for a laminar boundary-layer curve using the Blasius function and neglecting heat transfer. The theoretical error in the experimental X-ray absorption density measurements was calculated to be about ± 0.8 percent, which corresponds to a minimum detectable difference in air density of 6×10^{-4} pound per cubic foot. Each point was obtained from three 1-minute determinations. The experimental points appear to establish a common trend, indicated by the dashed line, with an accuracy better than the calculated accuracy. This common trend of the X-ray density runs indicates the potentialities

of the X-ray absorption method for boundary-layer density evaluations even in cases similar to the present one, where the flow conditions are extremely unfavorable for any density-gradient determinations.

The one station boundary-layer curve of density ρ against the distance y from the surface of the model was obtained by reading the X-ray intensity and by subsequently calculating the density ρ for each measured distance y. In order to eliminate the tedious procedure of data reading and point-by-point calculation, a recorder computer was developed that can plot the changing air densities directly as a function of a linear scale, which in the case of a boundary-layer determination would be the y-scale (see appendix B).

Operating characteristics required when using X-ray equipment with Geiger-Mueller counters and photographic film for air-density measurements in a boundary layer of an airfoil at given flow conditions are calculated in appendix C.

EFFECT OF DIVERGENT X-RAY BEAM ON BOUNDARY-LAYER EVALUATIONS

An X-ray beam consists of bundles of divergent rays due to the mode of propagation of X-rays. If the density is constant throughout the space encompassed by the X-ray beam, the absorption will be practically the same for divergent and parallel rays. If a density gradient exists throughout the space covered by a divergent beam, however, each ray will traverse layers of different density. This problem is encountered in the investigation of boundary layers by an X-ray absorption method.

The Machlett, Type A-2 Diffraction, tube has a focal spot of about 0.004 by 0.04 inch at the target as seen from the direction of the beryllium window. In the X-ray arrangement with the G-M counter as detector, the 0.002-inch slit sees the 0.004-inch wide X-ray beam entering the test section with a width of less than 0.003 inch and as if the X-rays would emanate from an array of point sources. In addition, an integrated intensity over the receiving-slit area represents each point measurement. The divergence of the rays therefore hardly affects the measured absorption in the case of point-by-point determinations provided the size of the detecting pickup is of the same order of magnitude as the beam probing the absorbing medium.

As for the single-exposure photographic method, the divergence of the beam poses a problem due to the large area of the detector of more than 0.25 inch in diameter. In addition, an integrated intensity over the exposure is no solution because all density changes to be investigated are contained in this area. The individual measurements are obtained by integrating over small areas, which are determined by the size of the densitometer pickup.

On the assumption that all rays diverge radially from a point X-ray source, which is directly adjacent to the entrance side of the test section, so that $d = L$, the air density through the traversed distance $r_{\varphi,\theta}$ is integrated by each X-ray at a given angle φ and θ from the center ray of the divergent beam. Then the emulsion density is a function of $r, \varphi,$ and θ and equation (10) for any constant angle φ and θ becomes

$$D_{\varphi,\theta} = -0.434\,\gamma \int_0^R B\rho(r_{\varphi,\theta})\,dr_{\varphi,\theta} + K' \tag{15}$$

Because the experimental emulsion densities $D_{\varphi,\theta}$ of the exposure are obtained as a function of the linear distance y from the model, it is desirable to obtain equation (15) in the same coordinates. For two-dimensional flow, $\rho(r_{\varphi,\theta})$ can be substituted by $\rho(y)$, $r_{\varphi,\theta} = (y-a)/\sin\varphi\cos\theta$, and $dr_{\varphi,\theta} = dy/\sin\varphi\cos\theta$, where a is the distance from the plate to the center of the X-ray beam, which is the center of the exposure. The length R of all $r_{\varphi,\theta}$ can be assumed to be constant and equal to the path length L; then

$$\cos\theta\sin\varphi \approx \frac{Y - a}{L}$$

where Y is the distance of $r_{\varphi,\theta}$ normal to the model at the location of the photographic material and equation (15) can be written

$$D_Y = -\frac{0.434\,\gamma L}{Y - a}\int_a^Y B\rho(y)dy + K \tag{16}$$

Differentiation with respect to the parameter Y gives

$$\frac{dD}{dY} = \frac{0.434\,\gamma L}{(Y - a)^2}\int_a^Y B\rho(y)dy - \frac{0.434\,\gamma LB\rho(Y)}{Y - a} \tag{17}$$

In order to determine the density $\rho(Y)$, equations (16) and (17) are combined to yield

$$\rho(Y) = -\frac{1}{0.434\ \gamma BI}\left[(Y - a)\frac{dD}{dY} + D - K'\right] \tag{18}$$

For the boundary condition, $Y = a$ and $\rho(Y) = \rho(a)$. Then equation (18) reverts to the parallel-beam relation given in equation (10);

therefore

$$K' = D_a + 0.434\ \gamma\ BL\rho(a) \tag{19}$$

The photographic exposure gives an emulsion density against distance (D against Y) curve. The derivative of that curve dD/dY is required to obtain the air-density distribution through the boundary layer, (equation (18)). The tangent dD/dY can be measured for each point by mechanical means and equation (18) can thus be plotted point by point. The accuracy of this procedure depends entirely on the scale to which the emulsion-density curve D against Y is drawn; therefore the boundary-layer curve, equation (18), can be obtained as accurately by this means as the experimental data permit. An empirical curve-fitting procedure would appear to be another plausible method of attacking the problem. For instance, by determining a differentiable power relation for the experimental emulsion density and distance curve, equation (18) can be used to calculate point-by-point air-density values.

When the X-ray source is not directly adjacent to the test section, so that $d > L$ (fig. 1), the density-distance equation becomes

$$\rho(Y) = \frac{L}{d}\rho(Y)_{18} + \left(1 - \frac{L}{d}\right)\rho(Y_1) \tag{20}$$

$$= \frac{L}{d}\rho(Y)_{18} + \frac{L}{d}\sum_{n=1}^{\infty}\left(1 - \frac{L}{d}\right)^n \rho(Y_n)_{18} \tag{21}$$

where $\rho(Y)_{18}$ is the density as given in equation (18) and $\rho(Y_1)$ is the density at the entrance points Y_1 where Y_1 is the distance measured at the X-ray entrance side to the absorber corresponding to Y. The entrance points Y_1 are related to the measured distances Y so that

$$Y_1 = \left(1 - \frac{L}{d}\right)Y + \frac{L}{d}a$$

The term $\rho(Y_n)_{18}$ denotes the densities as calculated from equation (18) for points $Y_1, Y_2, \ldots Y_n$, where

$$Y_n = \left(1 - \frac{L}{d}\right)Y_{n-1} + \left(\frac{L}{d}\right) a$$

Because the second factor of equation (21) in most cases is a rapidly converging series, the calculation of two to three terms will usually suffice.

CONCLUDING REMARKS

Commercial X-ray equipment with Geiger-Mueller counters as detectors was found adequate for measuring the densities within an accuracy of 6×10^{-4} pound per cubic foot in a tunnel of 4 inch width operating at near atmospheric density, where an X-ray-beam width of 0.002 inch and a measuring time of about 3 minutes were used. For a 1-minute measuring time, therefore, an accuracy in density measurement of 1.1×10^{-3} pound per cubic foot was obtained.

The X-ray technique of measuring density has been applied to a boundary layer of a flat plate at a station $7\frac{3}{8}$ inches from the leading edge and at a Mach number of 0.55.

For lower-density tunnels, higher X-ray intensities and softer X-rays are required to maintain the accuracy of the measurements. These requirements can be achieved by employing specially built, demountable X-ray tubes and by eliminating all window material.

For more efficient operation and production of a permanent record of the density measurements, a counting rate computer recorder was developed. Experiments have shown this instrument to be successful in plotting air densities directly as a function of a linear scale. In order to record the air densities through a boundary-layer station, the motion of the paper has to be coupled to the motion of the probing X-ray beam.

Commercial X-ray equipment with photographic film as a detector was found adequate for measuring the density in a 5.1-inch path length with an accuracy of about 4×10^{-4} pound per cubic foot when a densitometer pickup of 0.063-inch diameter was used, and with a microphotometer slit of 0.0004-inch width. An exposure time of less than 1 minute was employed in both cases.

Photographic material as the detector has the advantage over counting methods in that all desired data are obtained from one measurement. In addition, no movable parts are required for scanning.

The photographic method poses a problem, however, in that a correction for the divergence of the X-ray beam seems necessary when evaluating density gradients such as those encountered in boundary layers. Correction methods are suggested.

Lewis Flight Propulsion Laboratory,
National Advisory Committee for Aeronautics,
Cleveland, Ohio, March 7, 1951.

APPENDIX A

SYMBOLS

The following symbols are used in this report:

A	X-ray beam area at distance d
a	distance from airfoil to center of X-ray beam
B	total mass absorption coefficient
C	function of constant absorption in d - L
C'	proportionality constant
D	film emulsion density
D_a	film emulsion density at a
D_m	film emulsion density for $\rho = \rho_m$
D_Y	film emulsion density at Y
$D_{\varphi,\theta}$	film emulsion density at X-ray angle φ and θ
d	distance from X-ray source to detector
I	X-ray intensity after absorption
I_n	X-ray intensity at n kilovolts, n = 3.2, 4.0, 4.9, 6.8
I_0	initial X-ray intensity
i	inertia of film emulsion
K	proportionality constant, equation (5)
K'	proportionality constant, equation (10)
K"	proportionality constant, equation (10)
k	proportionality constant, equation (14)
L	absorber path length
M	Mach number

N	total measuring counts
N_B	total background counts
N_R	total reference counts
n	true counting rate
R	path length of diverging X-ray, $R \approx L$, $R \approx d$
R_m	measured counting rate
r,φ,θ	spherical coordinates with X-ray source at center
$r_{\varphi,\theta}$	path of X-ray divergent at angle φ and θ
S	absorption due to X-ray scattering
t	film exposure time
V	X-ray accelerating voltage
Y	distance from airfoil as measured on photographic film
Y_1	distance measured at X-ray entrance side to absorber corresponding to Y
y	distance from airfoil
Z	atomic number
γ	slope of characteristic film curve
ρ	air density
ρ_0	free-stream air density
ρ_B	air density at surface of model
ρ_m	maximum air density for each run in figure 5
$\rho(Y)$	air density as function of Y
τ	resolving time of Geiger-Mueller counter

APPENDIX B

RECORDER COMPUTER

The X-ray intensities are usually obtained as counts per unit time. Commercial counting-rate meters that record the integrated pulses over a fixed time are available; most commercial counting-rate meters, however, are unsuitable for problems where rapidly changing counting rates of randomly distributed pulses have to be recorded, because a relatively long time determination at each constant condition is necessary if the measurement is to be accurate within the relative probable error as given in equation (7). An instrument was therefore developed that measures the time required for a constant number of counts instead of the counting rate. This instrument has the added advantage that the relative probable error introduced by the statistical nature of the occurrence of the pulses remains fixed provided the background count is small compared with the measured count. The air density is then a direct function of the logarithm of the time required to permit the passage of the fixed number of pulses. For the developed apparatus, the amount of time for a given air density is proportional to the angle of rotation of a cylinder that carries a logarithmic spiral. The cylinder is stopped in its rotation almost instantaneously at the occurrence of the last of the predetermined number of pulses. Provisions are made for printing a record where the spiral touches the paper chart. After printing, the cylinder returns automatically and rapidly (in a few seconds) to its starting position to be ready for the next determination.

Air densities measured by the X-ray absorption method have thus been recorded and check well with the air densities calculated from pressure and temperature readings. When recorded X-ray densities are calculated back to intensities, they are practically in complete agreement with counting-rate readings taken simultaneously with the recordings. Hence, the recorder does not seem to introduce any noticeable additional inaccuracies into the air-density measurements.

For the experiments the paper chart moved on a ratchet arrangement. For boundary-layer evaluations, the motion of the paper will have to be coupled to the X-ray scanning mechanism.

APPENDIX C

SAMPLE CALCULATION

The practicability of the use of the X-ray-absorption method for air-density-gradient studies is demonstrated by the presentation of a typical boundary-layer problem encountered at the Lewis laboratory and the manner in which it would be treated using in turn the Geiger-Mueller counter and photographic film as receiver.

A supersonic wind tunnel embodying a flat-plate model has the following operating parameters:

Tunnel width, L, ft	3
Free-stream density, ρ_0, lb/cu ft	0.0374
Mach number, M	2.38
which gives a boundary-layer density ratio, ρ_B/ρ_0	0.47
yielding a value for the density at the model surface, ρ_B, lb/cu ft	0.0176

Employment of the G-M counter necessitates calculation of the minimum applied X-ray accelerating potential to yield a sufficient counting rate, at least above 500 counts per minute, at the maximum density of the boundary layer (ρ_0).

A preliminary calculation using equation (2) and previously obtained data revealed that a mass absorption coefficient of approximately 30 square feet per pound is needed for the desired counting rate at the given operating conditions of the 3-foot tunnel. A study of both figures 2 and 3 indicates that a voltage of 4.9 kilovolts, in a stable operating region, corresponds to a mass absorption coefficient of 27.0 square feet per pound. Hence a sample calculation is shown for an accelerating potential of 4.9 kilovolts.

Under previously described experimental conditions and for an X-ray voltage of 3.2 kilovolts,

$$I_{3.2} = \frac{I_0}{4\pi d^2} CAe^{-B\rho L} = 1700 \text{ (counts/min)}$$

for

$$A = (0.002)\times(0.25) \text{ (sq in.)}$$

$$d = 9.1 \text{ (in.)}$$

$$B = 90 \text{ (sq ft/lb)}$$

$$\rho = 0.0730 \text{ (lb/cu ft)}$$

$$L = 4.0 \text{ (in.)}$$

The relative intensity ratio $I_{4.9}/I_{3.2}$ determined from figure 2 is about 9. Then under the same conditions,

$$I_{4.9} = \frac{I_0}{4\pi d^2} CAe^{-B\rho L} = 9 \times I_{3.2} = (9)\times(1700) \text{ (counts/min)}$$

yielding

$$\left(I_0 \frac{CA}{4\pi}\right)_{4.9} = \frac{9 \times 1700\ d^2}{e^{-B\rho L}} = \frac{9 \times 1700 \left(\frac{9.1}{12}\right)^2}{0.112} = 78{,}000 \text{ (counts/min)}$$

for the specified tunnel conditions of

$$d = 41.1 \text{ (in.)}$$

$$B = 27.0 \text{ (sq ft/lb)}$$

$$L = 3.0 \text{ (ft)}$$

equation (2) at 4.9 kilovolts becomes

$$I_{4.9} = \frac{78{,}000}{\left(\frac{41.1}{12}\right)^2} e^{-81\rho} = 6660\ e^{-81\rho}$$

For the maximum density, $\rho_0 = 0.0374$ (lb/cu ft)

$$I_{4.9} = 6660\ e^{-3.03} = (6660)\times(0.049)$$

$$= 326 \text{ (counts/min)}$$

Because this number of counts is below that minimum previously specified, the use of a larger slit is suggested. A 1/2-inch slit gives about 650 counts per minute and is assumed for the following calculations.

For the minimum density $\rho_B = 0.0176$ pound per cubic foot,

$$I_{4.9} = (2)\ 6660\ e^{-0.143} = (2)\times(6660)\times(0.867)$$

$$= 11{,}560\ (\text{counts/min})$$

For the lowest counting rate of 650 counts per minute and a reference counting rate of 5000 counts per minute, the statistical error, calculated from equations (7) and (8), is approximately ±3.1 percent; hence

$$\left(\frac{\Delta I}{I}\right)_{max} = \pm 0.031$$

For the given boundary layer from $\rho_0 = 0.0374$ pound per cubic foot to $\rho_B = 0.0176$ pound per cubic foot using a 0.002- by 0.5-inch receiving slit, the minimum sensitivity is calculated from equation (3).

$$\left(\frac{d\rho}{\rho}\right)_{min} = \frac{\pm 0.031}{27(0.0176)\times(3)} = \pm 2.2\ (\text{percent})$$

The density change over the entire boundary layer $(\rho_0 - \rho_B)$ is 0.0198 pound per cubic foot; then the detectable density change, as calculated from equation (4), is less than ±2 percent of the entire density range of the boundary layer.

In order to determine the feasibility of using the X-ray photographic method for the given tunnel, the optimum combination of sensitivity and exposure time must be calculated. The mass absorption coefficient B best suited for the given operating conditions can be obtained from equation (12), where in this case ΔD is the useful range in emulsion densities from 0.7 to 1.1 if the microphotometer is to be used for the measurements of emulsion density.

Then

$$B = \frac{\Delta D}{(\rho - \rho_B)\ 0.434\gamma L} = \frac{0.4}{(0.0198)\ (0.434)\gamma L} = 9.3\ (\text{sq ft/lb})$$

Examination of figures 2 and 3 shows that this mass absorption coefficient corresponds to an accelerating voltage of about 6.8 kilovolts and is in a stable operating range for the X-ray equipment.

The exposure time $t_{6.8}$ is calculated by utilizing the fact that the energy (Ixt) remains constant for a fixed level of emulsion density. Thus

$$t_{6.8} = t_{4.0} \frac{(I_0)_{4.0}}{(I_0)_{6.8}}$$

And making use of equation (2),

$$t_{6.8} = t_{4.0} \frac{(I_0)_{4.0}}{(I_0)_{6.8}} \left(\frac{d_{6.8}}{d_{4.0}}\right)^2 \frac{e^{-(B\rho L)_{4.0}}}{e^{-(B\rho L)_{6.8}}}$$

where the subscripts 4.0 and 6.8 refer to the parameters used with the experimental test chamber and the given tunnel, respectively. The initial X-ray-beam intensity ratio $(I_0)_{4.0}/(I_0)_{6.8} = 1/7.5$, which is obtained from figure 2. The exposure time $t_{4.0}$ has been experimentally determined, as shown in figure 4, to be 30 seconds for $D = 0.7$.

A substitution of the given numerical values into the preceding equation leads to the following result for the exposure time:

$$t_{6.8} = 30 \left(\frac{1}{7.5}\right)\left(\frac{41.1}{9.1}\right)^2 \frac{e^{-(46.6)\ (0.073)\left(\frac{5.1}{12}\right)}}{e^{-(9.3)\ (0.0374)\ (3)}}$$

$$= 55 \text{ (sec)}$$

The minimum sensitivity is determined from equation (11)

$$\left(\frac{d\rho}{\rho}\right)_{min} = \frac{dD}{0.434\ \gamma BL\rho} = \frac{\pm 0.006}{(0.434)\ (1.66)\ (9.3)\ (0.0176)\ (3)} = \pm 2.1 \text{ (percent)}$$

REFERENCES

1. Arnold: Dichtemessungen mit Röntgenstrahlen an Uberschallströmungen im Windkanal. Archiv Nr. 66/124, Aerodynamisches Inst., Peenemünde Heeresversuchsstelle, Nov. 1, 1944.

2. Arnold: Density Tests on the Structure of Compression Shocks on Wedge-Profiles. Trans. of WVA Rep. Archive No. 192, by Lockheed Aircraft Corp.

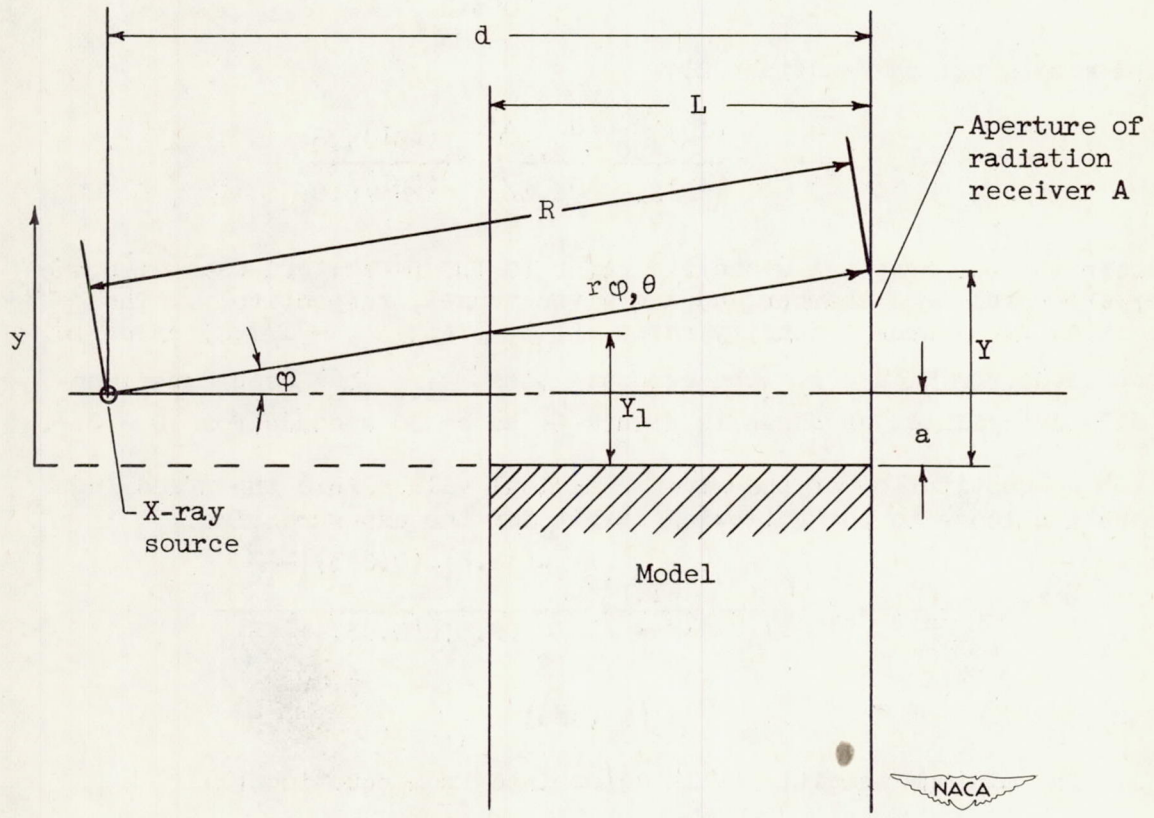

Figure 1. - Schematic diagram of setup.

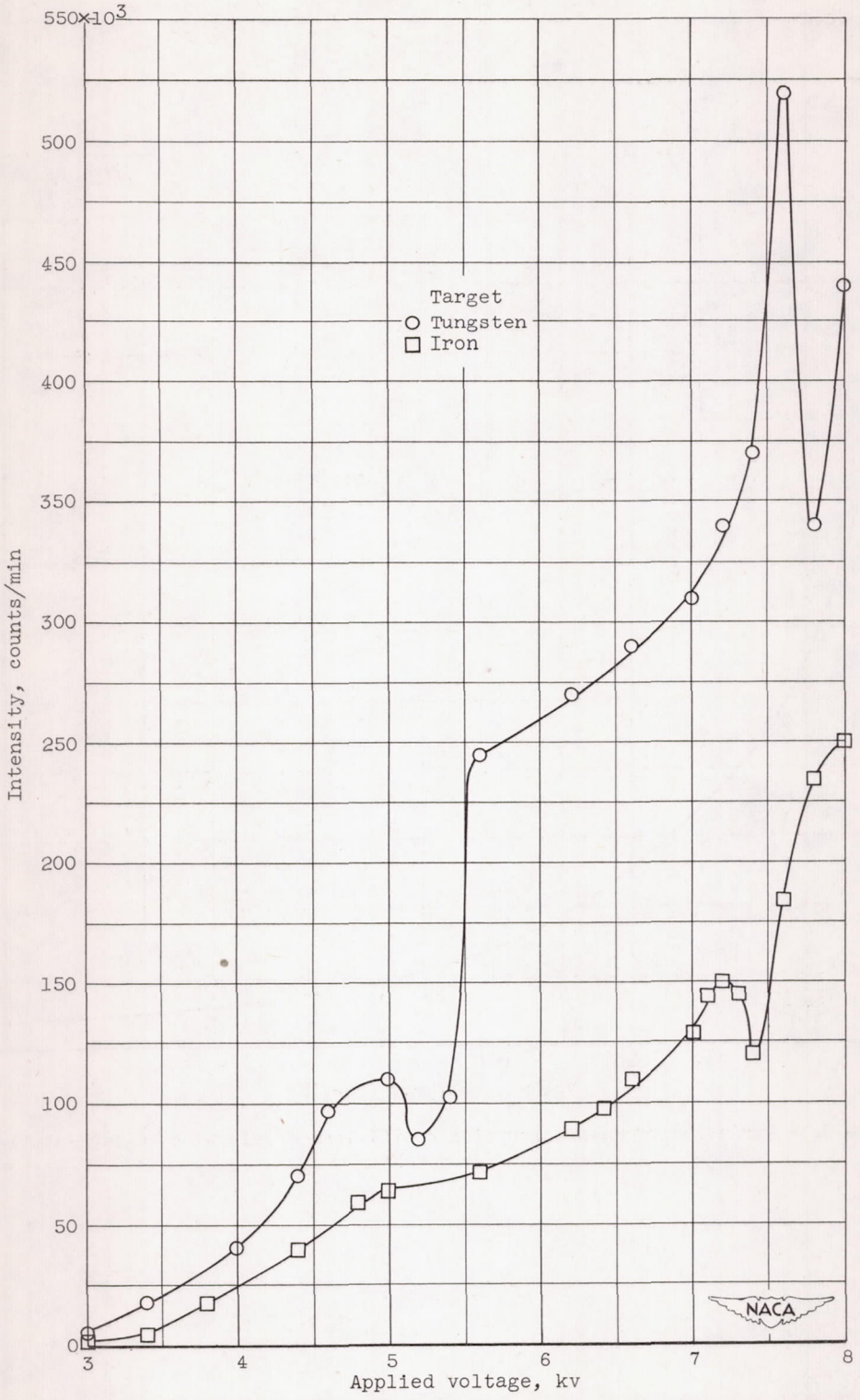

Figure 2. - Variation of X-ray-beam intensity with applied tube voltage. Plate current, 17.5 milliamperes.

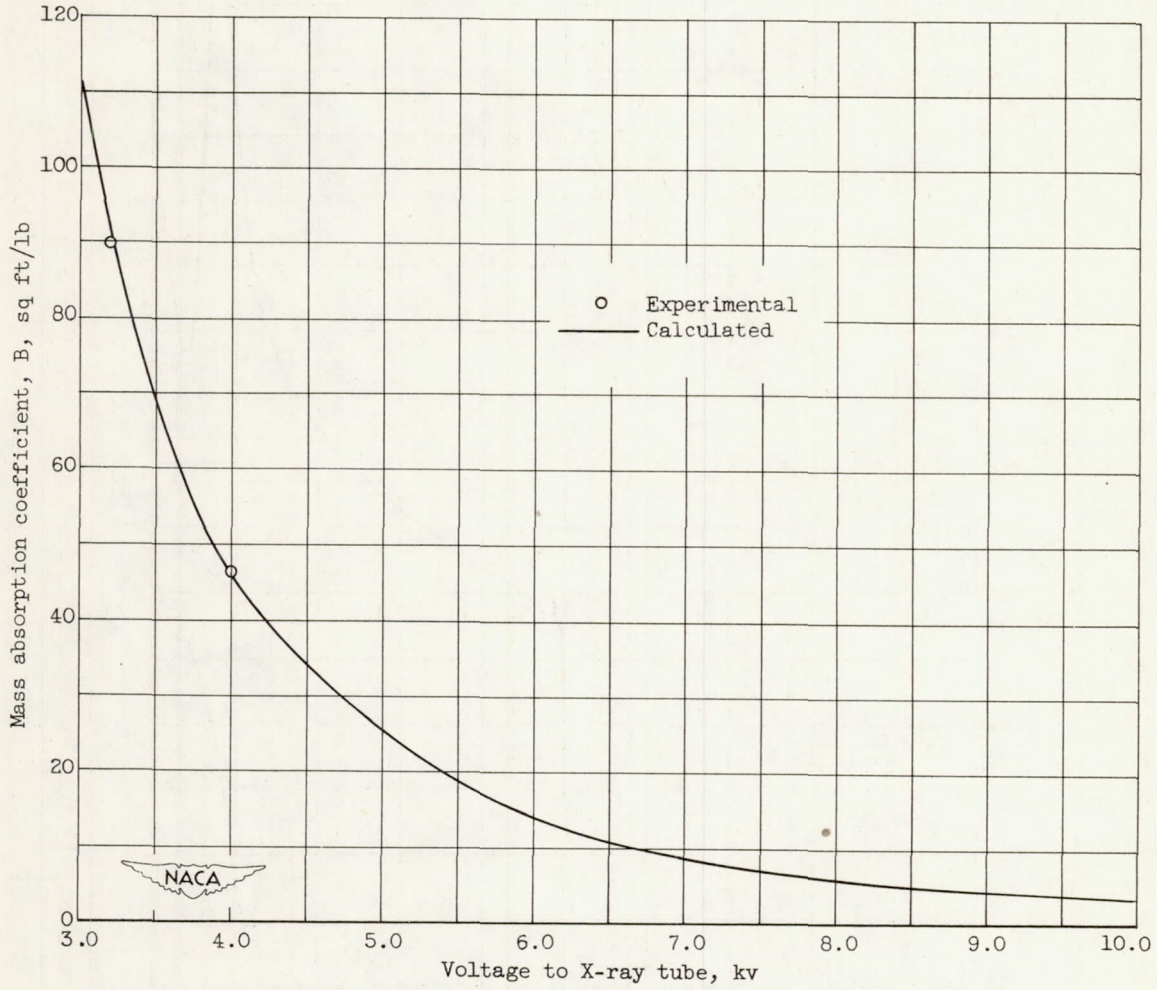

Figure 3. - Variation of mass absorption coefficient of air with voltage applied to X-ray tube.

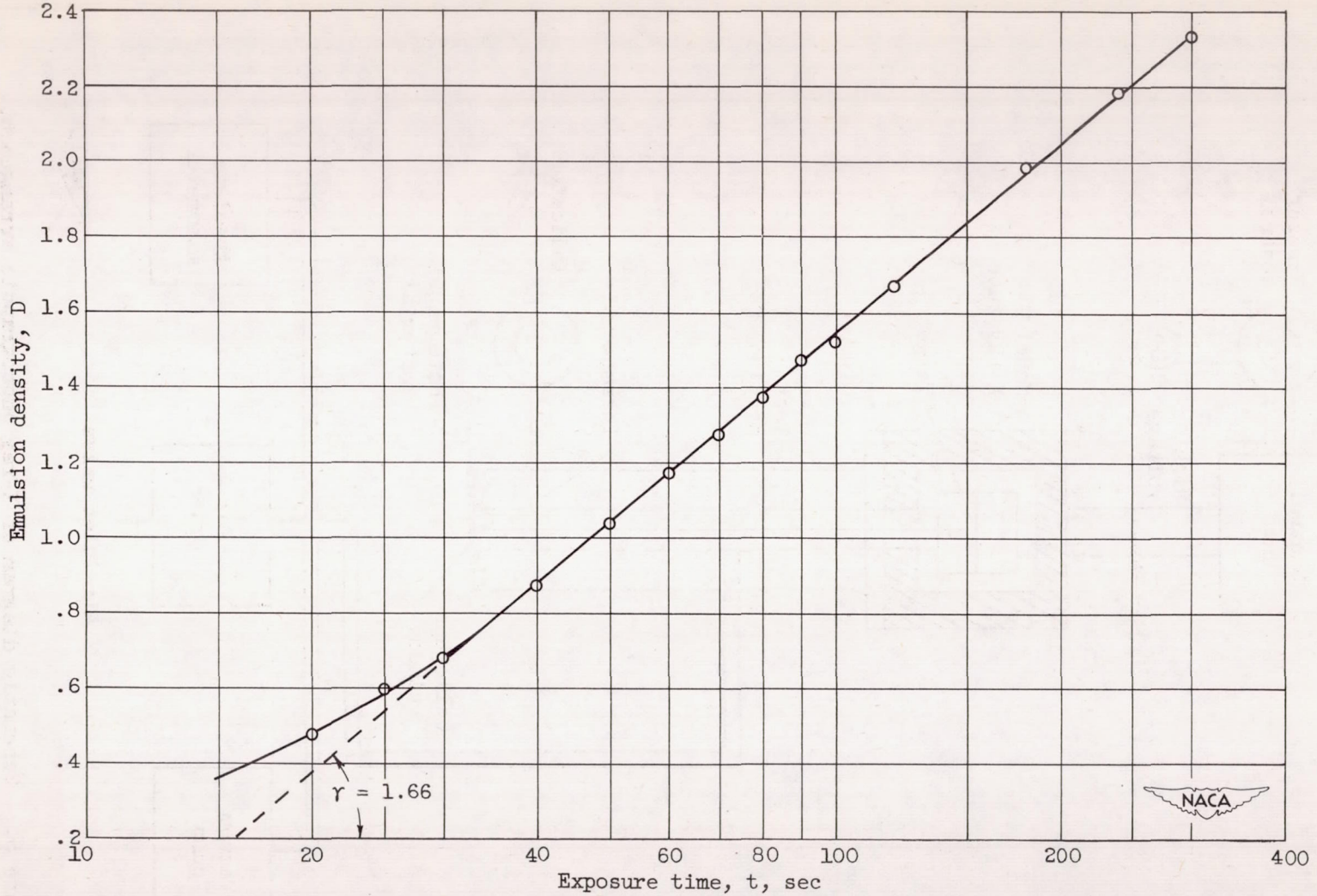

Figure 4. - Characteristic curve for Kodak film Spectrum Analysis No. 1. X-ray voltage, 4.0 kilovolts; current, 17.5 milliamperes; air density, ρ, 0.073 pound per cubic foot.

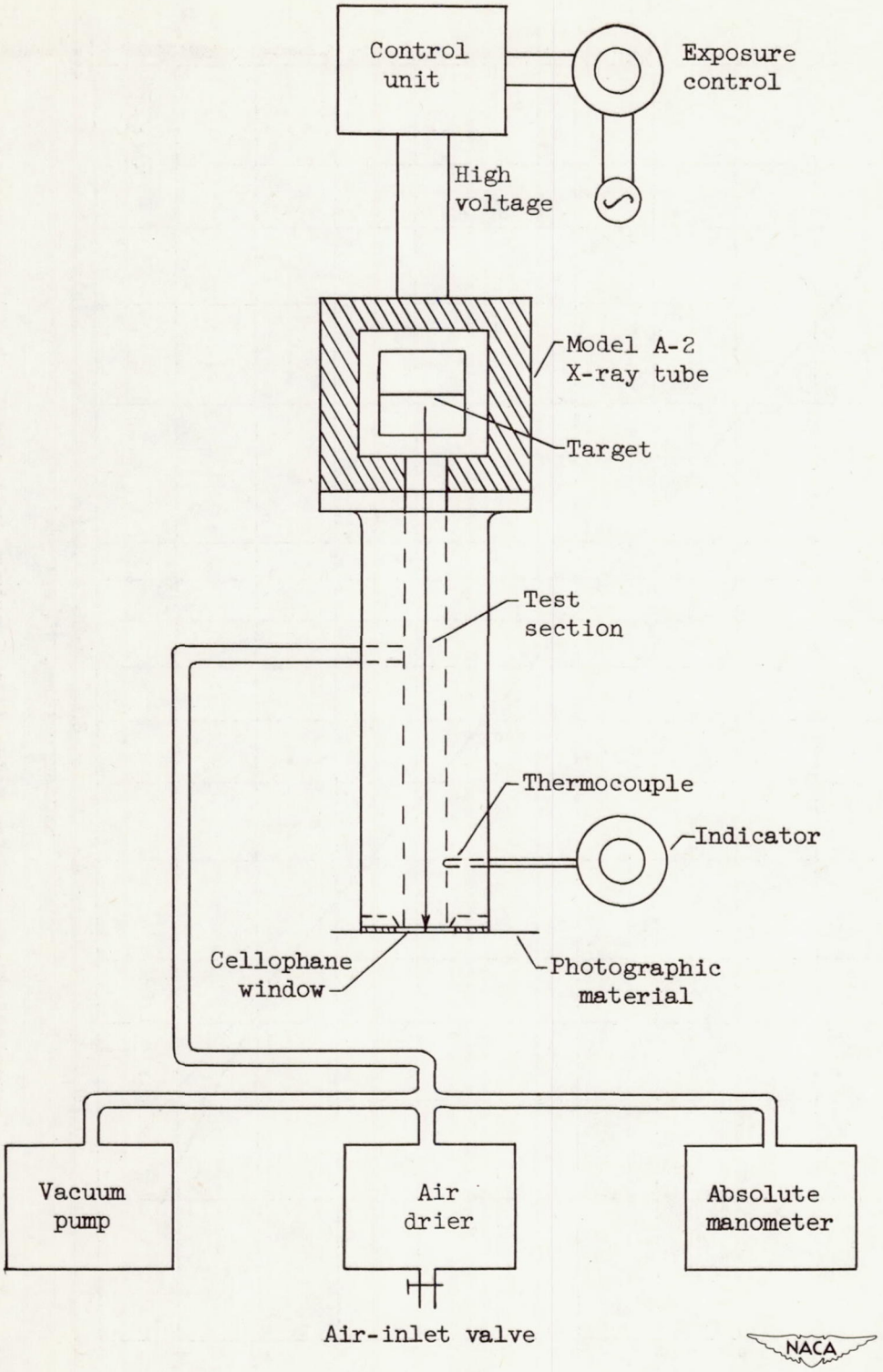

Figure 5. - Schematic diagram of X-ray photographic arrangement.

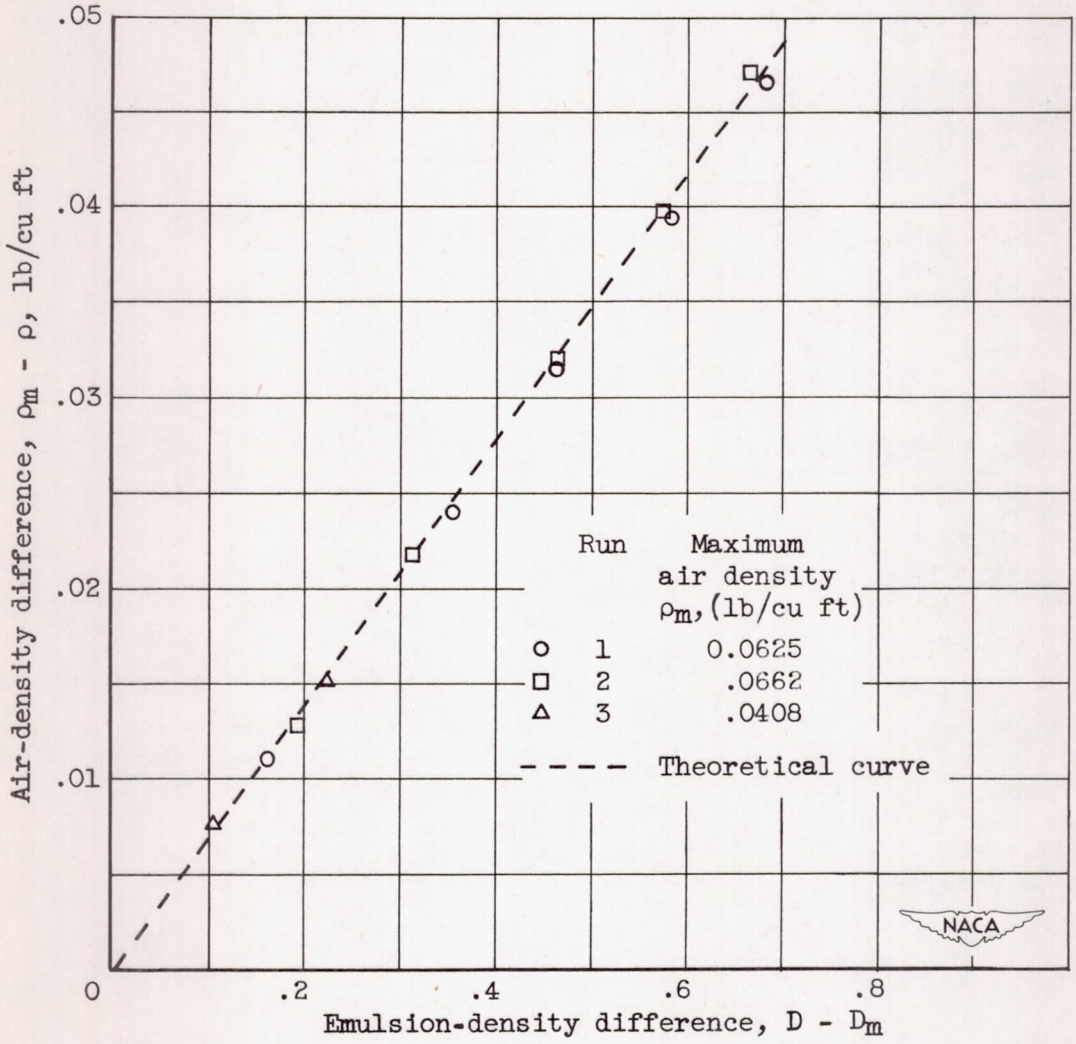

Figure 6. - Difference in air density as a function of emulsion density. Probable mean error in $D - D_m$, ±0.008.

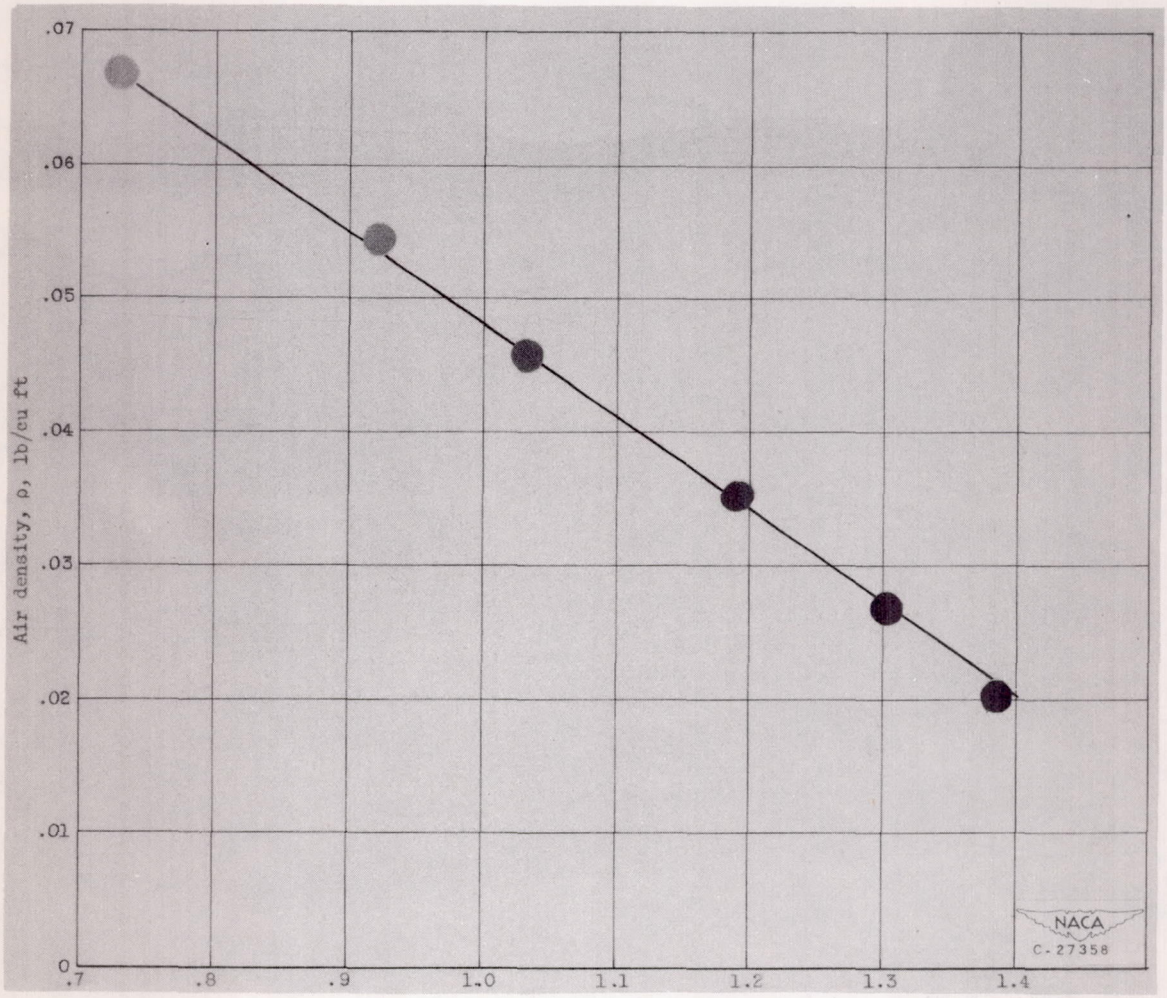

Figure 7. - Air density against emulsion density. (Representation of run 2 from fig. 6.)

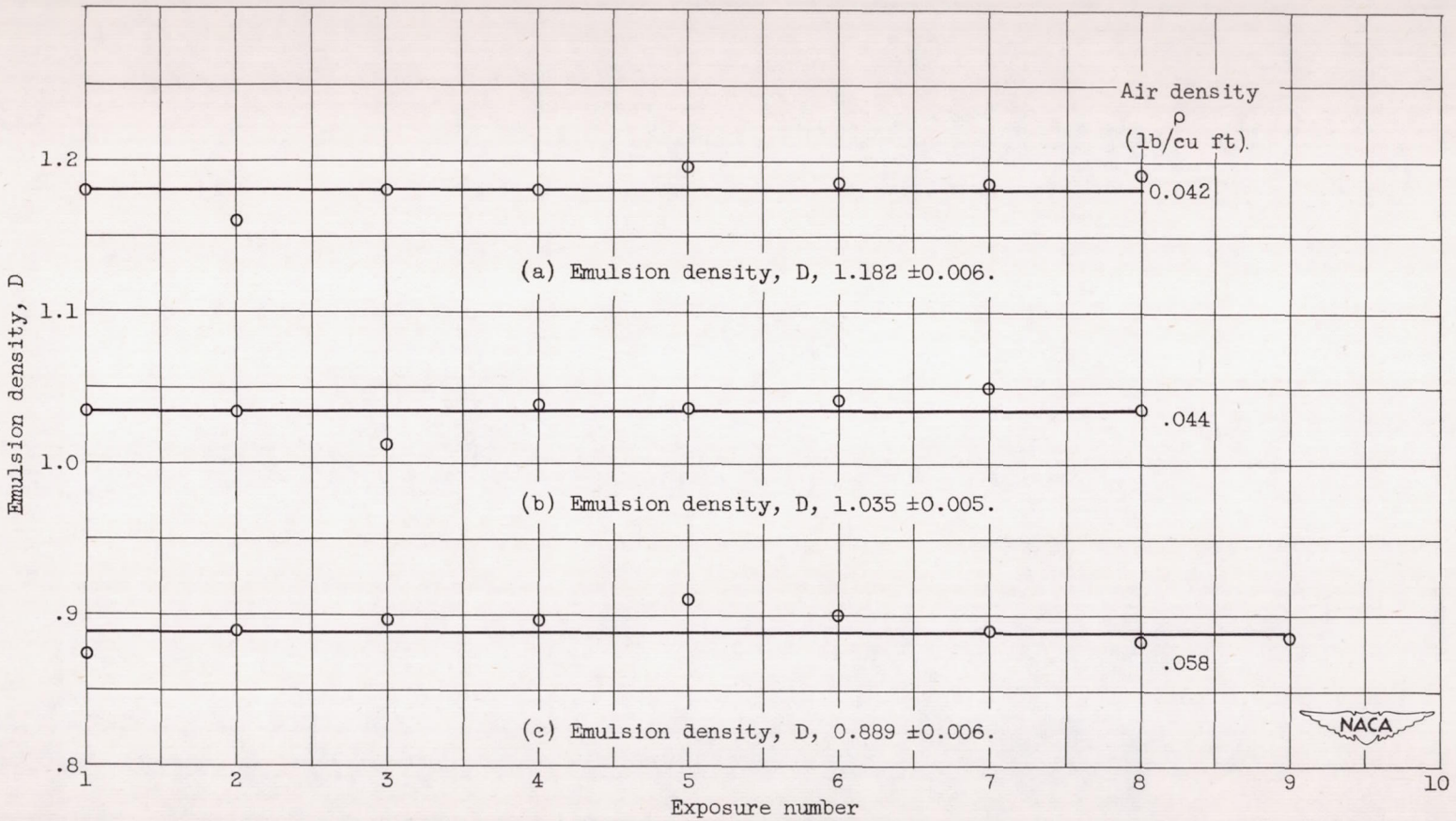

Figure 8. - Emulsion-density reproducibility at 4.0 kilovolts, 17.5-milliampere plate current, and 45-second exposure. Average ΔD, ±0.0055.

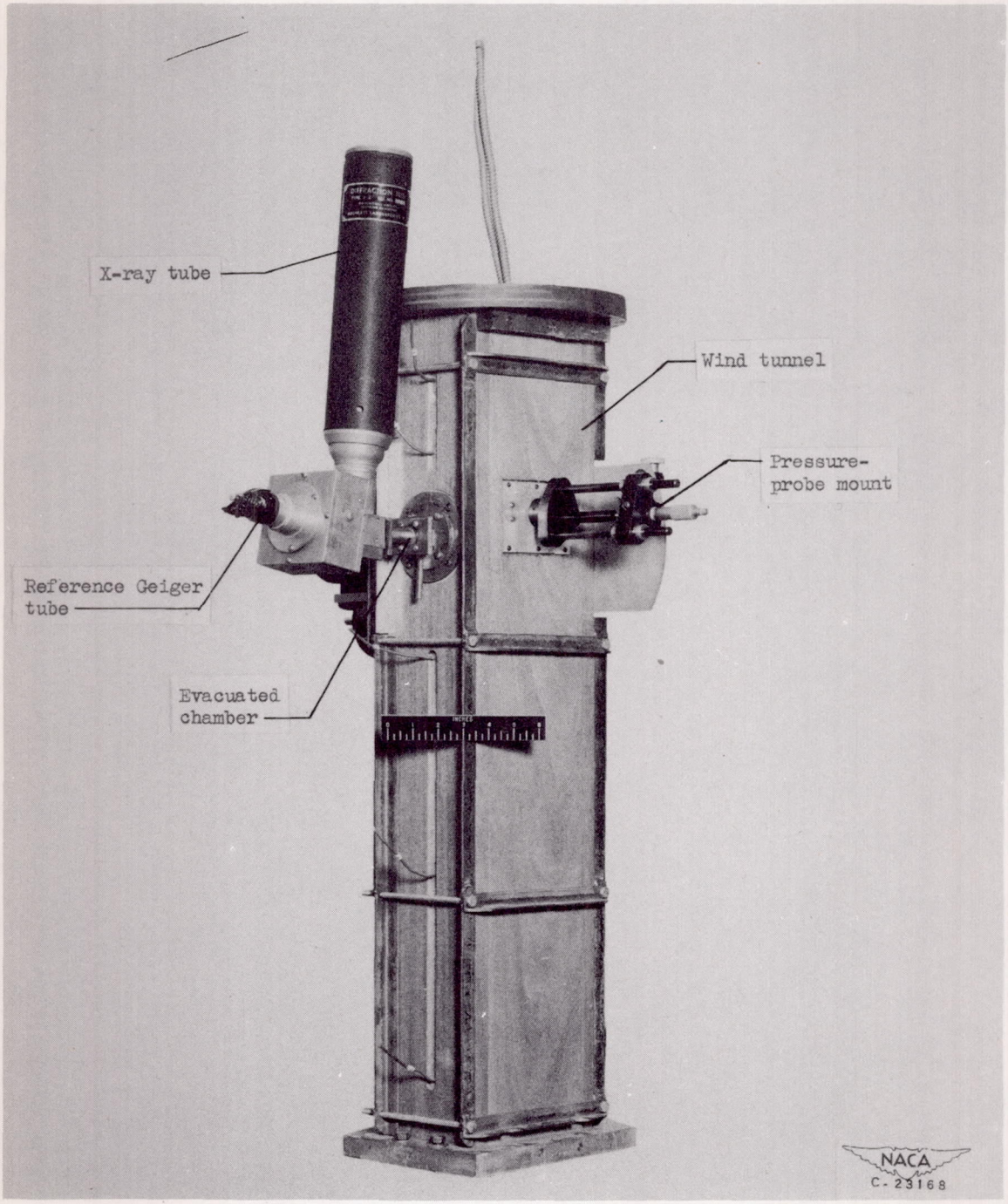

(a) X-ray beam entrance side.

Figure 9. - Tunnel section with X-ray equipment and associated parts.

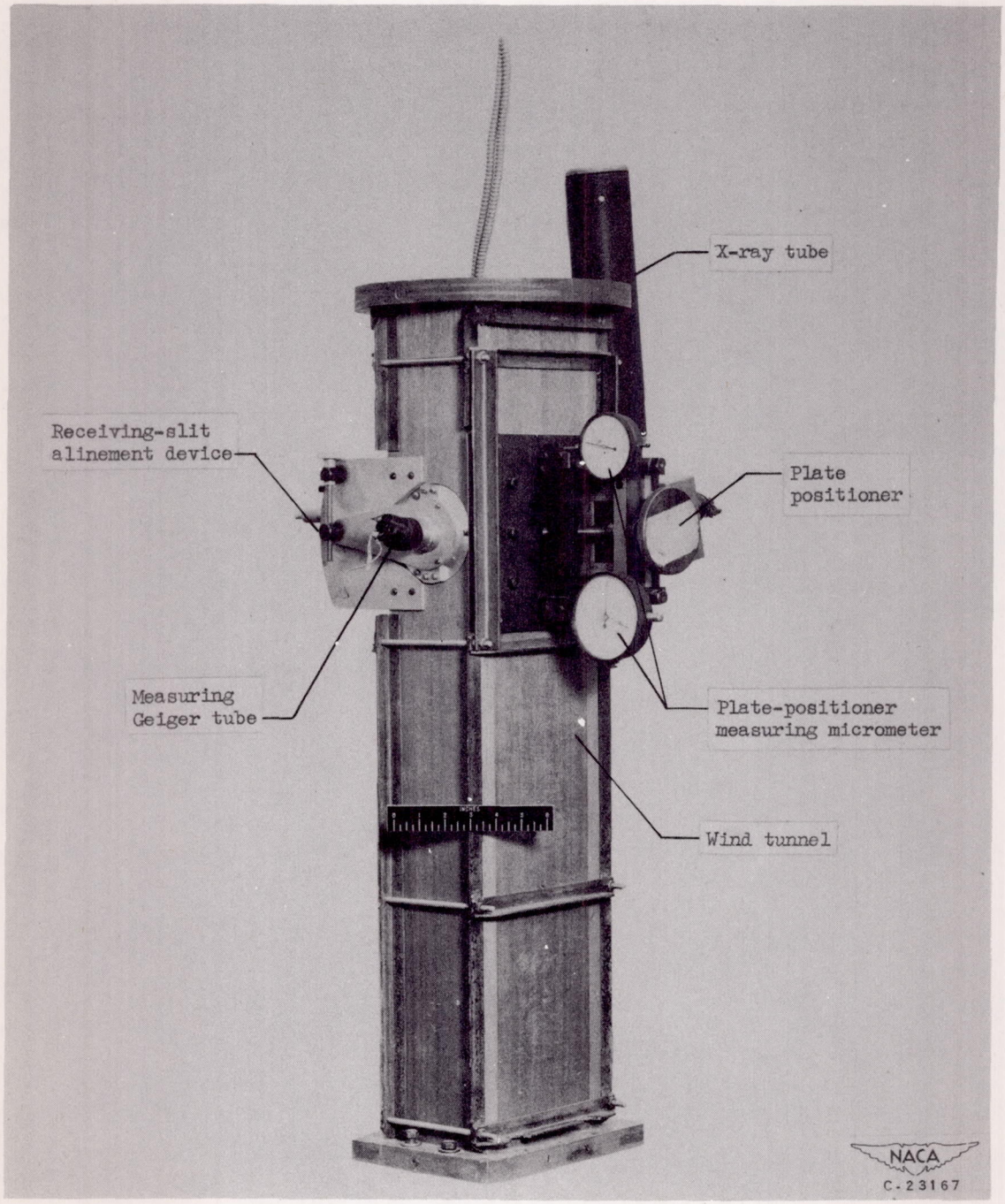

(b) X-ray beam exit and receiving side.

Figure 9. - Concluded. Tunnel section with X-ray equipment and associated parts.

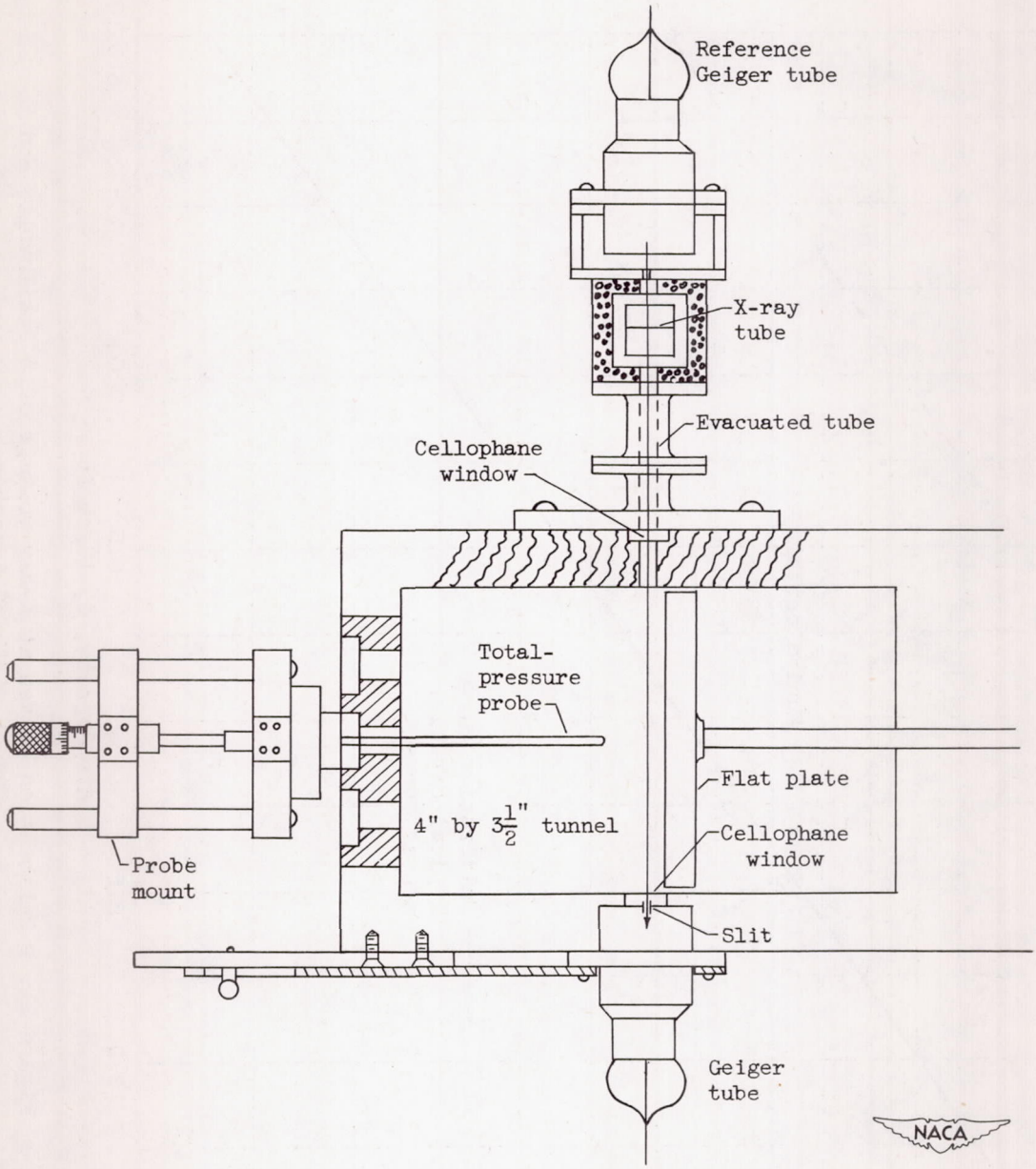

Figure 10. - Cross section of tunnel.

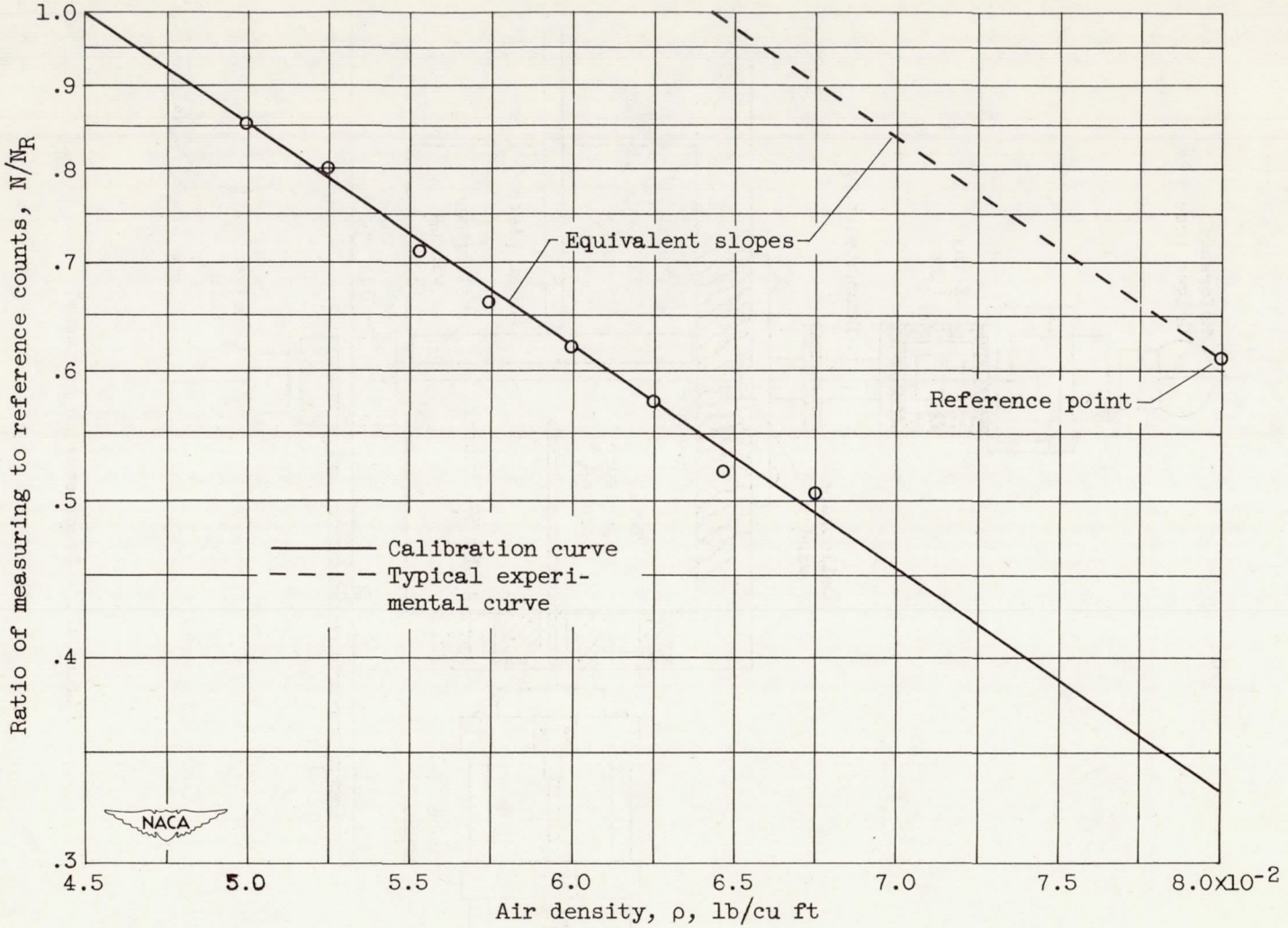

Figure 11. - Calibration curves at X-ray voltage of 3.2 kilovolts and tunnel width of 4 inches.

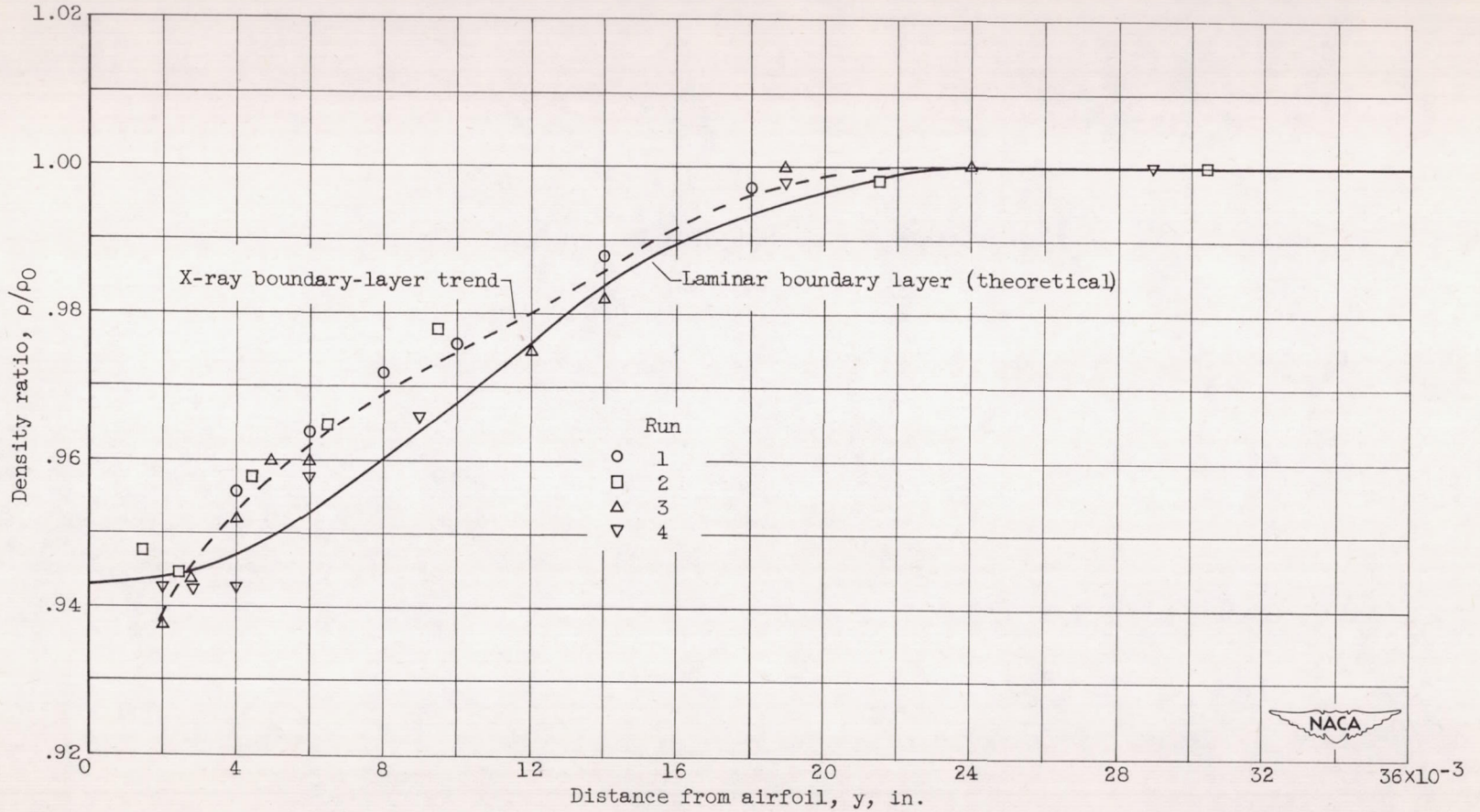

Figure 12. - Variation of density ratio with distance from model. Mach number, 0.55; Reynolds number, 2.46 x 10^6.